

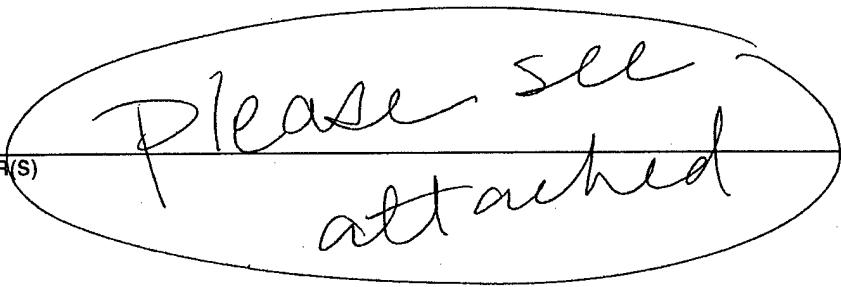
# REPORT DOCUMENTATION PAGE

Form Approved  
OMB No. 0704-0188

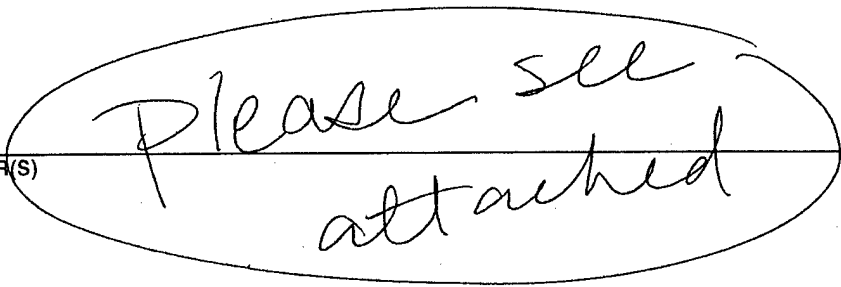
Public reporting burden for this collection of information is estimated to average 1 hour per response, including the time for reviewing instructions, searching existing data sources, gathering and maintaining the data needed, and completing and reviewing this collection of information. Send comments regarding this burden estimate or any other aspect of this collection of information, including suggestions for reducing this burden to Department of Defense, Washington Headquarters Services, Directorate for Information Operations and Reports (0704-0188), 1215 Jefferson Davis Highway, Suite 1204, Arlington, VA 22202-4302. Respondents should be aware that notwithstanding any other provision of law, no person shall be subject to any penalty for failing to comply with a collection of information if it does not display a currently valid OMB control number. PLEASE DO NOT RETURN YOUR FORM TO THE ABOVE ADDRESS.

1. REPORT DATE (DD-MM-YYYY)	2. REPORT TYPE Technical Papers	3. DATES COVERED (From - To)
-----------------------------	------------------------------------	------------------------------

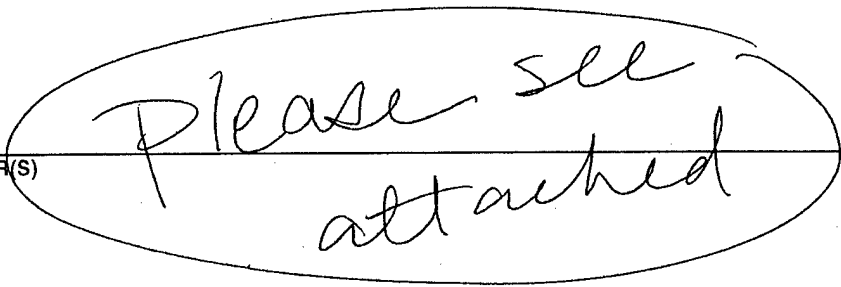
4. TITLE AND SUBTITLE	5a. CONTRACT NUMBER
-----------------------	---------------------

	5b. GRANT NUMBER
---	------------------

	5c. PROGRAM ELEMENT NUMBER
---	----------------------------

	5d. PROJECT NUMBER 2303
---	----------------------------

	5e. TASK NUMBER M2C8
---	-------------------------

	5f. WORK UNIT NUMBER 345709
---	--------------------------------

7. PERFORMING ORGANIZATION NAME(S) AND ADDRESS(ES)	8. PERFORMING ORGANIZATION REPORT
--	-----------------------------------

Air Force Research Laboratory (AFMC) AFRL/PRS 5 Pollux Drive Edwards AFB CA 93524-7048	
---	--

9. SPONSORING / MONITORING AGENCY NAME(S) AND ADDRESS(ES)	10. SPONSOR/MONITOR'S ACRONYM(S)
---	----------------------------------

Air Force Research Laboratory (AFMC) AFRL/PRS 5 Pollux Drive Edwards AFB CA 93524-7048	11. SPONSOR/MONITOR'S NUMBER(S) please see attached
---	--

12. DISTRIBUTION / AVAILABILITY STATEMENT
---


Approved for public release; distribution unlimited.
--

13. SUPPLEMENTARY NOTES
-------------------------

14. ABSTRACT
--------------

20030129 217

15. SUBJECT TERMS
-------------------

16. SECURITY CLASSIFICATION OF:			17. LIMITATION OF ABSTRACT 	18. NUMBER OF PAGES	19a. NAME OF RESPONSIBLE PERSON Leilani Richardson
a. REPORT Unclassified	b. ABSTRACT Unclassified	c. THIS PAGE Unclassified			19b. TELEPHONE NUMBER (include area code) (661) 275-5015

MEMORANDUM FOR PRS (In-House/Contractor Publication)

FROM: PROI (STINFO)

06 Sep 2001

SUBJECT: Authorization for Release of Technical Information, Control Number: **AFRL-PR-ED-TP-2001-182**  
Robert J. Hinde (Univ. of Tennessee); David T. Anderson (Univ. of Wyoming); Simon Tam; Mario E. Fajardo, "Probing Quantum Solvation W/ IR Spec.: IR Activity Induced in Solid pH<sub>2</sub> by N<sub>2</sub> and Ar Dopants"

Physical Review Letters  
(Deadline: ASAP)

(Statement A)

1. This request has been reviewed by the Foreign Disclosure Office for: a.) appropriateness of distribution statement, b.) military/national critical technology, c.) export controls or distribution restrictions, d.) appropriateness for release to a foreign nation, and e.) technical sensitivity and/or economic sensitivity.

Comments: \_\_\_\_\_  
\_\_\_\_\_  
\_\_\_\_\_

Signature \_\_\_\_\_ Date \_\_\_\_\_

2. This request has been reviewed by the Public Affairs Office for: a.) appropriateness for public release and/or b) possible higher headquarters review.

Comments: \_\_\_\_\_  
\_\_\_\_\_  
\_\_\_\_\_

Signature \_\_\_\_\_ Date \_\_\_\_\_

3. This request has been reviewed by the STINFO for: a.) changes if approved as amended, b) appropriateness of references, if applicable; and c.) format and completion of meeting clearance form if required

Comments: \_\_\_\_\_  
\_\_\_\_\_  
\_\_\_\_\_

Signature \_\_\_\_\_ Date \_\_\_\_\_

4. This request has been reviewed by PR for: a.) technical accuracy, b.) appropriateness for audience, c.) appropriateness of distribution statement, d.) technical sensitivity and economic sensitivity, e.) military/national critical technology, and f.) data rights and patentability

Comments: \_\_\_\_\_  
\_\_\_\_\_

APPROVED/APPROVED AS AMENDED/DISAPPROVED

\_\_\_\_\_  
PHILIP A. KESSEL Date  
Technical Advisor  
Space and Missile Propulsion Division

Best Available Copy

# Probing quantum solvation with infrared spectroscopy: infrared activity induced in solid parahydrogen by N<sub>2</sub> and Ar dopants

Robert J. Hinde\*

*Department of Chemistry, University of Tennessee, Knoxville, Tennessee 37996-1600*

David T. Anderson

*Department of Chemistry, University of Wyoming, Laramie, Wyoming 82071-3838*

Simon Tam<sup>o</sup> and Mario E. Fajardo

*U.S. Air Force Research Laboratory, AFRL/PRSP, Edwards Air Force Base, California 93524-7680*

We present high-resolution infrared absorption spectra of solid parahydrogen matrices containing low concentrations of N<sub>2</sub> or Ar impurities. The spectra reveal dopant-induced absorption features that acquire infrared activity through short-range isotropic vibrational transition dipole moments arising from dopant--H<sub>2</sub> intermolecular interactions. These dopant-induced features provide new insights into the perturbation of the vibron bands of the H<sub>2</sub> matrix by chemical impurities, and thus into the physics of solvation in a quantum solid.

DOI: fauxPRL.doc

PACS numbers: 33.20.Ea, 67.80.-s, 78.30.-j

Solid hydrogen and its isotopomers (HD and D<sub>2</sub>) have long been recognized as unique cryogenic media for high-resolution spectroscopic studies of molecular rovibrational dynamics in condensed phases [1,2]. In the lowest energy state of the solid H<sub>2</sub> crystal, solid parahydrogen (pH<sub>2</sub>), each H<sub>2</sub> molecule is in its  $j=0$  rotational state and is therefore a spherically symmetric object with no electrostatic multipole moments. Consequently, the pH<sub>2</sub> crystal is bound together only by weak pH<sub>2</sub>--pH<sub>2</sub> dispersion interactions, making solid pH<sub>2</sub> a very "soft" and nearly non-perturbing environment for molecular impurities. This has motivated recent high-resolution infrared (IR) absorption studies [2-4] of the rovibrational spectra and dynamics of dopants embedded in solid pH<sub>2</sub> matrices. Analysis of these spectra within the framework of crystal field theory provides valuable information on dopant--pH<sub>2</sub> interactions and on the microscopic nature of dopant trapping sites in the pH<sub>2</sub> matrix.

Complementary information can be obtained by investigating the impurity-induced changes in the IR absorption spectrum of the H<sub>2</sub> matrix itself. For instance, pH<sub>2</sub> solids containing low concentrations of  $j=1$  orthohydrogen (oH<sub>2</sub>) rotational "impurities" exhibit an IR absorption feature near 4153 cm<sup>-1</sup> that is assigned to the pure vibrational Q<sub>1</sub>(0) transition ( $v=1 \leftarrow 0$ ,  $j=0 \leftarrow 0$ ) of pH<sub>2</sub> molecules in the matrix [5]. Although this transition is strictly IR inactive in isolated gas phase pH<sub>2</sub> molecules and in pure solid pH<sub>2</sub>, orientational transitions of the oH<sub>2</sub> dopant's permanent quadrupole moment provide a mechanism for inducing nonzero Q<sub>1</sub>(0) transition moments in pH<sub>2</sub> molecules within the doped solid [6]. This oH<sub>2</sub>-induced absorption feature has a characteristic asymmetric lineshape arising from "vibron hopping," or delocalization

of the  $v=1$  vibrational excitation throughout the pH<sub>2</sub> matrix. Analysis of this lineshape provided important information on the vibrational dependence of the H<sub>2</sub>--H<sub>2</sub> potential before the era of *ab initio* and molecular beam studies of intermolecular potentials [6-8].

Spherical dopants such as alkali metal and rare gas atoms can also induce IR activity in solid pH<sub>2</sub> matrices [9], although via a qualitatively different mechanism that originates in short-range isotropic overlap-induced transition dipole moments [10] arising from intermolecular exchange interactions. The effectiveness of this induction mechanism stems from the fact that a chemical impurity breaks the local symmetry of the pH<sub>2</sub> lattice; hence this mechanism is truly general, and applies to atomic and molecular impurities alike. Because the net transition moment for these induced transitions depends sensitively on the microscopic structure of the dopant trapping site [10], careful study of these spectral features can provide new insights into the nature of impurity solvation in the pH<sub>2</sub> quantum solid.

In this Letter, we report high-resolution investigations of the IR spectra of solid pH<sub>2</sub> matrices doped with N<sub>2</sub> impurities. Because both  $j=0$  and  $j=1$  N<sub>2</sub> rotational levels are populated in the cryogenic solid pH<sub>2</sub> environment, these doped matrices turn out to be good model systems for comparing the newly-identified isotropic induction mechanism with previously studied mechanisms based on transition dipoles induced by the electrostatic fields of impurity species. This is because the  $j=0$  N<sub>2</sub> dopants are spherical objects with no multipolar electrostatic field, and thus act only via the short-range isotropic mechanism to induce IR activity in adjacent H<sub>2</sub> molecules, while the  $j=1$  N<sub>2</sub> dopants (like oH<sub>2</sub> molecules) induce transition dipoles

in both nearby and distant  $\text{pH}_2$  molecules by virtue of their permanent quadrupole moments. Hence, two distinct induction mechanisms are active in a single sample.

We prepare millimeters-thick doped solid  $\text{pH}_2$  samples by rapid vapor deposition [9] of flows of precooled  $\text{H}_2$  gas and room temperature dopant gas onto a  $\text{BaF}_2$  substrate cooled to  $T \approx 2$  K by a liquid helium bath cryostat. The precooled  $\text{H}_2$  gas emerges from a variable temperature ortho/para  $\text{H}_2$  converter [11] typically operated at  $T \approx 15$  K to produce nearly pure  $\text{pH}_2$  gas flows with approximately 100 parts per million (ppm) of residual  $\text{oH}_2$ . In some cases we operate the converter at elevated temperatures to produce  $\text{oH}_2$ -enriched samples.

The absorption spectra of the doped  $\text{pH}_2$  samples are recorded along the substrate normal using a Fourier transform IR spectrometer. As-deposited spectra are recorded immediately after deposition at a substrate temperature of  $T \approx 2.4$  K. We then anneal the samples by raising the substrate temperature to  $T \approx 4.8$  K, and record some spectra at this temperature as well. Sample thicknesses are measured to within  $\pm 10$  % (95 % confidence level) using the approach described in Ref. 12. The impurity concentrations cited here are ratios of the quantities of dopant and  $\text{H}_2$  en-

tering the sample chamber. These values may differ from the actual impurity concentrations in the solid (due to varying sticking efficiencies of  $\text{pH}_2$  and dopant molecules, among other reasons) but are estimated to be within  $\pm 40$  % of the *in situ* concentrations.

Figure 1 shows the IR absorption spectra of four as-deposited  $\text{pH}_2$  samples. Trace (a) depicts the spectrum of a  $\text{pH}_2$  sample containing 10 ppm of  $\text{CH}_4$ , which is included in each sample as a structural tracer for monitoring the morphology of the as-deposited samples [3,4]. No detectable IR activity in the  $\text{pH}_2$   $Q_1(0)$  region is induced either by the  $\text{CH}_4$  dopant (at this concentration) or by the residual  $\text{oH}_2$  molecules present in the sample.

Trace (b) shows the absorption spectrum of solid  $\text{pH}_2$  containing 2500 ppm of  $\text{oH}_2$ , and displays both the  $\text{oH}_2$ -induced  $\text{pH}_2$   $Q_1(0)$  feature between  $4152$  and  $4153.2$   $\text{cm}^{-1}$  and the narrow  $Q_1(1)$  transition of the dopants themselves at  $4146.6$   $\text{cm}^{-1}$ . The  $Q_1(0)$  feature exhibits the asymmetric vibron hopping lineshape mentioned previously. This characteristic lineshape maps out the subset of delocalized  $Q_1(0)$  vibrons whose spatial wave functions achieve nonzero overlap with the quadrupolar electrostatic field of the  $\text{oH}_2$  dopant [6], and therefore indicates the presence of an induction mechanism based on quadrupole-induced transition moments.

Trace (c) depicts the spectrum of a  $\text{pH}_2$  sample containing 1000 ppm of natural isotopic abundance  $\text{N}_2$ ; it shows a broad, asymmetric absorption feature from about  $4150$  to  $4154$   $\text{cm}^{-1}$ . The position of this feature coincides closely with that of the  $\text{pH}_2$   $Q_1(0)$  transition observed in mixed  $\text{oH}_2/\text{pH}_2$  samples, and we assign this feature to  $\text{N}_2$ -induced  $Q_1(0)$  transitions of  $\text{pH}_2$  molecules in the doped solid.

The lineshape of this feature shares some common aspects with the  $\text{oH}_2$ -induced  $Q_1(0)$  feature shown in trace (b), including a relatively steep blue edge and a gently sloping red edge that meet at an absorption maximum at  $4153.1$   $\text{cm}^{-1}$ . Despite these similarities, we can rule out any possibility that the feature shown in trace (c) may arise from residual  $\text{oH}_2$  impurities, because the residual  $\text{oH}_2$  concentration in the  $\text{N}_2$ -doped sample is too low to produce the  $Q_1(1)$  feature seen at  $4146.6$   $\text{cm}^{-1}$  in the  $\text{oH}_2$ -enriched sample. Furthermore, the feature shown in trace (c) is much broader at the baseline than is the  $\text{oH}_2$ -induced  $Q_1(0)$  transition shown in trace (b). We therefore attribute the  $\text{N}_2$ -induced feature in trace (c) to the superposition of *two distinct*  $\text{N}_2$ -induced  $\text{pH}_2$   $Q_1(0)$  transitions: a quadrupole-generated feature induced by  $j=1$   $\text{N}_2$  dopants, which gives the central portion of the peak its characteristic shape, and a broader, unstructured feature induced by spherical  $j=0$   $\text{N}_2$  dopants.

Support for this interpretation is provided by trace (d) in Fig. 1, which depicts the IR spectrum of a  $\text{pH}_2$  sample containing 1000 ppm of Ar. The spherical Ar dopants induce a broad, structureless  $\text{pH}_2$   $Q_1(0)$  feature visible from

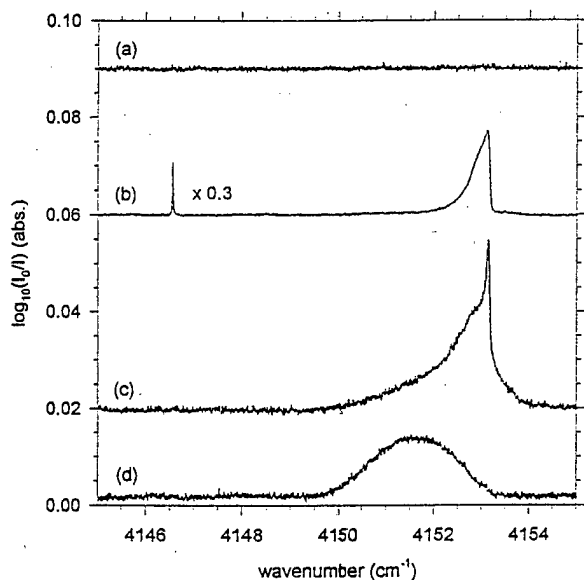


FIG. 1. Absorption spectra of four as-deposited doped  $\text{pH}_2$  solids at  $T \approx 2.4$  K. Trace (a) is for a sample containing 10 ppm of  $\text{CH}_4$ ; trace (b) is for a sample containing 10 ppm of  $\text{CH}_4$  and 2500 ppm of  $\text{oH}_2$ ; trace (c) is for a sample containing 10 ppm of  $\text{CH}_4$  and 1000 ppm of  $\text{N}_2$ ; trace (d) is for a sample containing 10 ppm of  $\text{CH}_4$  and 1000 ppm of Ar. Sample thicknesses are 2.7, 4.0, 3.1, and 2.9 mm for traces (a) through (d) respectively. Trace (b) has been scaled by a multiplicative factor of 0.3 to compensate for the higher dopant concentration and thickness of this sample. Traces (a) through (d) are presented at respective resolutions of 0.0075, 0.008, 0.01, and 0.008  $\text{cm}^{-1}$  and have been displaced vertically for ease of presentation.

4150 to 4153  $\text{cm}^{-1}$ , much like the underlying broad feature in trace (c) that we have attributed to  $j=0$   $\text{N}_2$  molecules. As we explain in more detail below, the lineshapes of spectral features attributed to the isotropic overlap induction mechanism differ from those of features arising from quadrupole induction because different subsets of the  $\text{pH}_2$  crystal's  $Q_1(0)$  vibrons are rendered IR active by the two mechanisms. This shows that careful study of these dopant-induced features can shed new light on the fundamental physics of the host  $\text{pH}_2$  matrix.

The  $Q_1(0)$  features we have attributed to the symmetry breaking isotropic induction mechanism originate in (vibrational) transition dipole moments induced by short-range intermolecular exchange interactions [10]. The same transition moments lead to collision-induced  $Q_1(0)$   $\text{H}_2$  IR absorption in pure  $\text{H}_2$  [13,14] and in gaseous mixtures of  $\text{H}_2$  with other atomic and molecular species [15], and the  $Q_1(0)$   $\text{pH}_2$  features induced by Ar and  $j=0$   $\text{N}_2$  dopants thus represent solid-phase analogues of collision-induced absorption. The "collisions" which generate overlap-induced transition moments in the  $\text{pH}_2$  matrix are simply intimate, short-range interactions between nearest-neighbor molecules in the solid. These nearest-neighbor interactions play an especially prominent role in solid  $\text{pH}_2$  matrices because the individual  $\text{pH}_2$  molecules in the solid undergo large-amplitude zero point motions about their nominal lattice sites [17]; this in turn amplifies the effects

of overlap-induced transition dipole moments, which decrease rapidly with increasing intermolecular distance [16].

Because these overlap-induced  $Q_1(0)$  transition moments depend strongly on the dopant- $\text{pH}_2$  distance, the transitions rendered IR active by spherical dopants are those in which the final state's  $Q_1(0)$  vibron has substantial amplitude on one or more of the twelve  $\text{pH}_2$  molecules which are adjacent to the dopant. (In addition, the final state's vibron wave function must have appropriate symmetry, so that the transition moment vectors associated with these twelve  $\text{pH}_2$  molecules do not sum to zero.) In contrast, the electrostatic field of  $\text{oH}_2$  and  $j=1$   $\text{N}_2$  dopants decays rather slowly with increasing distance (as  $1/R^4$ ), and the quadrupole induction mechanism therefore also activates vibrons with substantial amplitudes on non-nearest-neighbor  $\text{pH}_2$  molecules. Consequently, the spectral features induced by spherical dopants give us unique insight into the perturbation of the host crystal's vibron bands by chemical impurities, making them important tools for studying solvation in the  $\text{pH}_2$  matrix environment.

Our interpretation of trace (c) in Fig. 1 assumes that  $\text{N}_2$  dopants in solid  $\text{pH}_2$  retain good rotational quantum numbers. Evidence that this is so is provided in Fig. 2, which shows the temperature dependence of four satellite IR absorption features in the vicinity of the  $\text{N}_2$ -induced  $Q_1(0)$  feature. The strongest of these features is a multiplet that decreases in intensity upon heating, consisting of three peaks at 4162.3, 4163.2, and 4164.9  $\text{cm}^{-1}$ , each 0.9  $\text{cm}^{-1}$  wide. A weak structureless feature whose intensity is independent of temperature appears centered at 4170.6  $\text{cm}^{-1}$  and is 1.3  $\text{cm}^{-1}$  wide. Two very weak features, each about 4.2  $\text{cm}^{-1}$  wide, appear when the sample is heated to  $T \approx 4.8$  K: one is a doublet centered at 4142.1  $\text{cm}^{-1}$  and the other is a shoulder centered at 4178.5  $\text{cm}^{-1}$  superimposed on the the  $\text{pH}_2$   $Q_R$  phonon sideband. The spectral changes produced by heating the doped  $\text{pH}_2$  sample are fully reversible.

As we show next, the observed temperature dependence of these satellite features, and their positions relative to the sharp maximum of the  $Q_1(0)$  peak, indicate that they arise from cooperative transitions in which the  $\text{pH}_2$   $Q_1(0)$  transition is accompanied by a pure rotational  $\Delta j = 2$  transition of the  $\text{N}_2$  dopant. This demonstrates that  $\text{N}_2$  dopants rotate nearly freely in the  $\text{pH}_2$  matrix.

The homonuclear  $\text{N}_2$  molecule exists in ortho and para nuclear spin modifications associated with even and odd rotational quantum numbers, respectively [18]. In the absence of a catalyst, interconversion between orthonitrogen and paranitrogen is very slow; hence the even and odd  $j$  levels of  $\text{N}_2$  achieve thermal equilibrium independently in the cryogenic  $\text{pH}_2$  matrix. Although the rotational constant of  $\text{N}_2$  dopants in the matrix environment differs slightly from that of isolated gas phase  $\text{N}_2$  molecules (see below), this difference is small enough that we can esti-

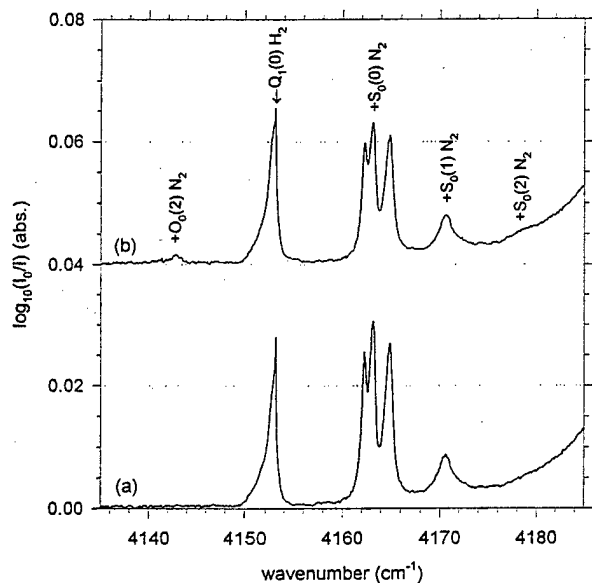


FIG. 2. Temperature dependence of the absorption spectra of the 3.1-mm-thick  $\text{N}_2/\text{pH}_2$  sample shown in trace (c) of Fig. 1. Trace (a) is as-deposited at  $T \approx 2.4$  K; trace (b) is recorded at  $T \approx 4.8$  K. Both spectra are presented at 0.1  $\text{cm}^{-1}$  resolution and have been displaced vertically for ease of presentation. The notations  $+S_0(j)$  and  $+O_0(j)$  represent cooperative transitions in which the  $\text{pH}_2$   $Q_1(0)$  vibrational excitation is accompanied by a pure rotational transition of the  $\text{N}_2$  dopant from the  $(v=0, j)$  state to the  $(v=0, j+2)$  and  $(v=0, j-2)$  states, respectively.

mate the rotational level populations of  $N_2$  dopants reasonably well using the gas phase rotational constant  $B_{\text{gas}} = 1.99 \text{ cm}^{-1}$  [19]. At  $T \approx 2.4 \text{ K}$  only the  $j=0$  and  $j=1$  levels of  $N_2$  are appreciably populated, with fewer than 0.5 % of the  $N_2$  molecules in levels with  $j \geq 2$ . Heating the sample to 4.8 K promotes approximately 15 % of the  $j=0$  molecules to the  $j=2$  level, but excites fewer than 1 % of the  $j=1$  molecules to the  $j=3$  level.

Consequently, the triplet feature shown in Fig. 2, which decreases in intensity by roughly 20 % upon heating, can be assigned to cooperative transitions which combine the  $Q_1(0)$   $pH_2$  excitation with  $S_0(0) \Delta j = 2$  transitions of the  $N_2$  dopant from its  $j=0$  level. The relative intensities of the three peaks remain constant during the annealing cycle, confirming that the peaks arise from a common initial state that is depopulated upon heating. The triplet nature of this feature suggests that interactions between the  $pH_2$  vibron and the  $N_2$  dopant's  $j=2$  rotational wave function lift the orientational degeneracy of the  $j=2$  state. Given the approximate 1:2:2 intensity ratio of the three components of the triplet, we assign the peaks at 4162.3, 4163.2, and 4164.9  $\text{cm}^{-1}$  to transitions to the  $m_j = 0, \pm 1$ , and  $\pm 2$  levels of the  $j=2$  state, respectively.

The weak features that appear only in the spectrum of the heated sample can be assigned to cooperative transitions involving  $\Delta j = \pm 2$  transitions from the  $N_2$   $j=2$  level, as indicated by the  $O_0(2)$  and  $S_0(2)$  labels in Fig. 2. This  $N_2$  rotational level becomes populated (at the expense of the  $N_2$   $j=0$  level) when the sample is heated to  $T \approx 4.8 \text{ K}$ . Conversely, the temperature-independent feature at 4170.6  $\text{cm}^{-1}$  arises from cooperative transitions involving  $S_0(1) \Delta j = 2$  transitions from the  $N_2$   $j=1$  level; the population of this  $N_2$  level is unaffected by the thermal cycling depicted in Fig. 2.

To confirm these rotational assignments, we note that the center of gravity of the  $oH_2$ -induced  $Q_1(0)$  feature [trace (b) in Fig. 1], at 4152.8  $\text{cm}^{-1}$ , marks the vibron-free origin of the quadrupole-induced  $Q_1(0)$  vibron band in solid  $pH_2$  [6]; this represents the energy required to excite a  $Q_1(0)$  transition localized on a single  $pH_2$  molecule in the solid. The centers of gravity of the  $N_2$ -induced satellite features are shifted from this band origin by amounts corresponding to the energies of the appropriate  $N_2$   $\Delta j = \pm 2$  rotational transitions, which are simply integer multiples of the  $N_2$  rotational constant  $B$  in the matrix environment: 6  $B$  for the  $S_0(0)$  and  $O_0(2)$  transitions, 10  $B$  for the  $S_0(1)$  transition, and 14  $B$  for the  $S_0(2)$  transition. Applying this analysis to the features shown in Fig. 2 yields  $B = 1.79 \pm 0.04 \text{ cm}^{-1}$ , which is reduced by 10 % from  $B_{\text{gas}} = 1.99 \text{ cm}^{-1}$  by crystal field effects. The good agreement among the rotational constants derived from the four satellite features indicates that the rotational assignments in Fig. 2 are internally consistent.

To summarize, we have presented high-resolution IR absorption spectra of  $N_2$ - and Ar-doped solid  $pH_2$ . The

dopant-induced features observed in the spectra provide information about the solvation of small dopants in the  $pH_2$  matrix and about the symmetry requirements and length scale of the induction mechanism generating the IR activity. In particular, the lineshapes of the dopant-induced features tell us which vibrons of the  $pH_2$  crystal are rendered active by a particular dopant, and how the crystal's vibron bands may be perturbed by the dopant's presence.

The information encoded in these dopant-induced IR absorption spectra can be extracted with the help of quantum Monte Carlo simulations [10] which account for the highly correlated, large-amplitude zero point motions of the  $pH_2$  solute molecules. Simulations of  $N_2$ -doped  $pH_2$  should enable a comprehensive analysis of the lineshapes and multiplet splittings of the  $N_2$ -induced spectral features, thereby shedding light on the rotational dynamics and solvation of chemical impurities in a highly quantum solid. Further work in this direction is in progress.

This work was completed while R.J.H. and D.T.A. were visitors at the Air Force Research Laboratory's Propulsion Sciences Division (Edwards AFB), supported through contracts administered by ERC, Inc. R.J.H. acknowledges additional support from the Air Force Office of Scientific Research (contract F-49620-01-1-0068) and from the Petroleum Research Fund.

\*Corresponding author. E-mail: rhinde@utk.edu

†Present address: KLA-Tencor Corporation,  
1 Technology Drive, Milpitas, CA 95035.

- [1] T. Oka, *Annu. Rev. Phys. Chem.* **44**, 299 (1993).
- [2] T. Momose and T. Shida, *Bull. Chem. Soc. Jpn.* **71**, 1 (1998).
- [3] T. Momose et al., *J. Chem. Phys.* **107**, 7707 (1997).
- [4] S. Tam et al., *J. Chem. Phys.* **111**, 4191 (1999).
- [5] H.P. Gush et al., *Can. J. Phys.* **38**, 176 (1960).
- [6] V.F. Sears and J. van Kranendonk, *Can. J. Phys.* **42**, 980 (1964).
- [7] J. van Kranendonk, *Can. J. Phys.* **38**, 240 (1960).
- [8] J. van Kranendonk and G. Karl, *Rev. Mod. Phys.* **40**, 531 (1968).
- [9] M.E. Fajardo and S. Tam, *J. Chem. Phys.* **108**, 4237 (1998).
- [10] R.J. Hinde, in *Proceedings of the High Energy Density Matter (HEDM) Contractors Conference*, Park City, Utah, October 2000 (unpublished).
- [11] S. Tam and M.E. Fajardo, *Rev. Sci. Instrum.* **70**, 1926 (1999).
- [12] S. Tam and M.E. Fajardo, *Appl. Spectrosc.* (submitted for publication, 2001).
- [13] H.L. Welsh, M.F. Crawford, and J.L. Locke, *Phys. Rev.* **76**, 580 (1949).
- [14] A.R.W. McKellar, *J. Chem. Phys.* **92**, 3261 (1990).
- [15] M.F. Crawford, H.L. Welsh, J.C.F. MacDonald, and J.L. Locke, *Phys. Rev.* **80**, 469 (1950).
- [16] G. Birnbaum, M.S. Brown, and L. Frommhold, *Can. J. Phys.* **59**, 1544 (1981).
- [17] I.F. Silvera, *Rev. Mod. Phys.* **52**, 393 (1980).
- [18] G. Herzberg, *Molecular Spectra and Molecular Structure. I. Diatomic Molecules*, reprint ed. (Krieger, Malabar, FL, 1989).
- [19] J. Bendsen, *J. Raman Spectrosc.*, **2**, 133 (1974).